

Phase transitions and critical phenomena of tiny grains thin films synthesized in microwave plasma chemical vapor deposition and origin of ν_1 peak

Mubarak Ali^{a,*}, I-Nan Lin^b

^a Department of Physics, COMSATS Institute of Information Technology, Islamabad 45550, Pakistan.

^b Department of Physics, Tamkang University, Tamsui Dist., New Taipei City 25137, Taiwan (R.O.C.).

*corresponding address: mubarak74@comsats.edu.pk, mubarak74@mail.com, Ph. +92-51-90495406

Abstract –Different trends have been observed in Raman spectroscopy and field emission characteristics of tiny grains carbon films known as nanocrystalline and ultra-nanocrystalline diamond films. Carbon atoms in solid state evolve structure of tiny grains either graphite or amorphous depending on the field force behavior and characteristics photons. Those tiny grains of carbon film evolved into graphitic phase following by elongation under the process of synergy, they modified into smooth elements while travelling photons of hard X-rays, are the origin of ν_1 peak in the Raman spectrum. Those tiny grains which retained two-dimensional structure are the origin of ν_2 peak. Tiny grains originated ν_1 peak having level of intensity low and those recorded signals at very high level of intensity reveal different modified phases known in exceptional hardness where origin of formation of diamond and lonsdaleite is the atomic hydrogen and for graphene is the atomic oxygen. Enhanced field emission characteristics of films resulted on the basis of tiny grains which were modified into smooth elements where propagation of photonic current accelerated. On interacting laser beam to tiny grains carbon film, resulted Raman signals was at different wave numbers revealing the same trend as in the case of energy loss spectroscopy.

Keywords: Tiny grains carbon films; Dynamics; Field force; Phase transitions; Raman spectra; Field emission characteristics; Energy loss spectroscopy

Introduction:

Phase transition of evolving structure is crucial as it may be the origin of a new phenomenon. Development of selective materials and investigating their characteristics at nanoscale, atomic and electronic level requires a new sort of observations. Wherever, dynamics influence the process, evolution of structure in different phases may be anticipated despite the fact that comprised atoms are belong to the same element. Again, a particularly developing structure of carbon atoms when in solid state may undergo various sorts of modification owing to process of synergy. Additionally, where atoms carry certain nature of electron states, their evolving structure may recognize certain phase, existing at nanoscale, depending on the mode of modification.

A large number of publications have been published on the syntheses of nanocrystalline diamond (NCD) and ultrananocrystalline diamond (UNCD) films at varying process conditions and their development mainly involve technique known as chemical vapor deposition (CVD). Performances of NCD/UNCD films are mainly recognized through microscopic observations, Raman spectroscopy, field emission characteristics and energy loss spectroscopy. The NCD/UNCD films mainly deal tiny grains size in few tens of nanometer to few nanometers. In a technique known as hot filament CVD, tiny grains of carbon were made as well prior to go for sticking at substrate, thus, may influence the phase of a particular evolving structure resulting into switch it to another phase [1].

It is absolute necessary to understand dynamics of tiny particles' formation prior to go for assembling into extended size particles [2]. Agglomerations of colloidal matter envisage atoms and molecules to deal them as materials for tomorrow [3]. Formations of different tiny particles have been discussed elsewhere [4]. The formation mechanism of tiny shaped particles has been discussed under certain concentration of gold precursor [5]. Under identical process parameters, the nature of precursor directs tiny shaped particles following by large shaped particles [6]. Different tiny shaped particles were developed under the 'tailored energy-shape photons' while varying the ratio of bipolar pulse OFF to ON time [7]. Triangular-shaped tiny particles synthesized directly under unipolar pulse ON/OFF time and a

particular structure evolved under the joint application of characteristic photon and a field force [7]; one at a time. Formation process of large-sized particles reveals very high development rate and tiny-sized particles which didn't attain uniform drive revealing diffusion prior to their compact packing [8]. A monolayer tiny particle in connecting triangles is under the tailored energy photon shape like tiny particle itself where it divides into two equal triangular-shaped tiny particles under the application of field force [5-8]. In all suitable metals and semimetals, the binding of atoms takes place under photon couplings [9]. Tiny shaped particle dealing localized gravity at solution surface along with modification into smooth elements have been discussed elsewhere [10]. Atoms of suitable elements execute electronic transitions do not ionize, deform or elongate, while inert gas atoms split under the application of photonic current [11]. The phenomena of heat and photon energy have been discussed while dealing silicon atom where under application of electron rest energy is being transformed into force energy [12]; heat energy at shunt level enables an electron to free from the force of its nucleus to go into excited state under levitational force and de-excitation of that electron is under the gravitational force of nucleus involving inertia at each stage of changing state, thus, electron configured 'force energy' shape like Gaussian distribution under the trajectory. Why some atoms are in gaseous state and some in solid state but carbon work on either side have been discussed elsewhere [13]. Under normal conditions, certain nature atoms of tiny particles deal deformation and elongation behavior at greater extent, therefore, may deal with either effective nanomedicine use or defective nanomedicine use [14].

Electron field emission (EFE) device fabricated by heating tiny diamond grains in hydrogen plasma reveals high characteristic and is due to high defect density and low electron affinity [15]. Increasing nitrogen content slightly increases sp^2 -bonding in grain-boundary and local bonding structure remains the same [16]. Diverse geometries coupled with varieties of attachment sites enabling diamondoids as useful building blocks for molecular-design applications [17]. Size of grains in UNCD film in the range of 2-3 nm remains thermodynamically stable as tested under broad range of pressure –temperature of hydrogenated surfaces [18]. Grains in nanometer size indicate specific changes because of the decreased mobile dislocations and below their critical size, a softening behavior is often observed and change is triggered by atomic shuffling where simulations approaches are incapable to evaluate underlying mechanism [19]. Sumant *et al.* [20] investigated the surface

chemistry and nanotribology inside the UNCD films and are indistinguishable chemically, adhesively and tribologically from single-crystal diamond.

Several studies on UNCD films are available in the literature targeting field emission characteristics under different process parameters and gases concentrations/dopants. On increasing the local density of states UNCD films provide conducting path at diamond-vacuum interface [21]. UNCD films synthesized at low temperatures and in nitrogen environment demonstrated high conductivity in their various applications [22]. Under nitrogen atmosphere, the grain size of UNCD film becomes smaller than 10 nm and metallic conductivity is achieved [23]. UNCD film has low friction/wear and rapid passivation of dangling bonds is a matter of concern in humid environment [24]. UNCD films are different as compared to NCD films in several ways such as their grain sizes are 2 nm to 5 nm, they are bound by sp^2 -carbon and usually grow in argon-rich/hydrogen-poor CVD environment and may contain 95–98% sp^3 -bonded carbon [25]. In UNCD films, homojunction facilitates the tunneling of electrons in conduction band and their direct transport at conducting/insulating interface [26]. To synthesize diamond films at temperatures below 600°C, UNCD films are superior in choice because, their properties don't degrade as in polycrystalline diamond films [27]. On increasing substrate temperature along with hydrogen concentration in Ar/CH₄ plasma sp^3 -diamond phase becomes less passivated [28]. Low friction coefficient of UNCD films is linked with large amounts of hydroxylic/carboxylic functional groups which are recognized as grain boundary [29]. Bias enhanced nucleation/growth processes facilitate the transport of graphitic phase in both interior and interface regions of UNCD films [30]. Hydrogen concentration increases the size of diamond grains [31]. Boron-doped UNCD films are capable of being utilized in the field of atomic force microscopy/robust electrodes/bio-compatible sensors [32]. On lowering the a-C layer at interface UNCD/Au-Si composite structure delivers better conductivity and improves EFE [33]. Precise growth of sub-2 nm/above 5 nm sized diamond grains is achieved due to energetic species under low growth temperature and pre-nucleated interface, thus, tiny grains on silicon nanoneedles deliver enhanced EFE [34]. Gold-UNCD films show superior EFE properties than copper-UNCD films and authentic factor underneath the mechanism is the presence of nanographitic phases [35]. Copper ion implantation and annealing process increase the EFE due to improved conducting nature of UNCD films [36]. Presence of graphitic phases at the interfaces

of ZnO nanorods/UNCD needles decreases the resistivity of layer and core-shell heterostructures, thus, delivered superior EFE [37]. Nitrogen-incorporated UNCD grains serve as 'high-density diamond nuclei' in the hybrid carbon film [38]. In all the above studies and many others not cited here, factors related to performance of UNCD/NCD films are linked with the tiny grains of UNCD/NCD films. Improvement in the conductivity but not EFE of P-ions incorporated-UNCD films was due to the transportation of electrons crossing interface [39]. Transportation of electrons is the prime reason for enhanced conductivity and emission properties of doped UNCD films [40].

Now, in the various published studies of NCD/UNCD films, they reveal elongation of tiny grains as well as deformation of their atoms, in some cases, and it is hard to recognize atoms in original shape as shown by the images of high resolution microscopy. Then various spectroscopic spectra of 'tiny grains carbon films', which are synthesized only under the slight variation of the parameters, reveal a range of peaks at varying intensity and shape along with different values of obtained data taken by various analyses and measurement tools. Principally, such carbon films should not only deal master structure (graphitic phase) and amorphous structure of tiny grains but also modified phases of tiny grains, both artificial and natural sorts of modifications, depending on the coordination of atomic hydrogen or atomic oxygen under certain scope of their electron states while in the process of synergy. It is anticipated that under coordination of electron state of atomic hydrogen and viable electron states of atomic oxygen to the unfilled ones of carbon atoms, one at a time, may result into different modified phase of tiny grains while occupying certain regions of 'tiny grains carbon film'. In addition to such modifications, where tiny grains evolve into two-dimensional structure don't modify under above-said coordination, but they may elongate either under the process of synergy or impinging electron streams of splitted atoms, thus, may modify into smooth elements in a large amount while travelling photons of hard X-rays at their surfaces as in the case of gold and silver tiny particles [4-8]. These provide strong incentive to re-investigate the process of development of 'tiny grains carbon films' known as UNCD/NCD films and identification of different phases along with performance of films under varying process conditions.

In the present work, different 'tiny grains carbon films', which are known as NCD and UNCD films, are synthesized in a technique known as microwave plasma

enhanced (MPE) CVD. Formation process of 'tiny grains carbon films' is discussed under the variation of chamber pressure along with different concentration of hydrogen gas. The evolution of graphite structure along with amorphous structure is also discussed. To modify a large amount 'graphitic phase tiny grains' into smooth elements is also discussed as well. In addition to modifications of graphitic phase tiny grains into smooth elements and their modifications into different phases, known in exceptional hardness, are discussed as well by pinpointing. Spectra of Raman spectroscopy and energy loss spectroscopy of 'tiny grains carbon films' synthesized at different chamber pressure tally along with field emission characteristics. The performance of carbon films in terms of specific phase of tiny grains has been discussed by pinpointing. In addition to those, confusion has been going on since three decades regarding the origin of peak related to ' ν_1 band' in Raman spectra and it was considered to be due to the size of the grains or the presence of transpolyacetylene layers around tiny grains. Present study indicates the real reason of peak related to ' ν_1 band'.

We envisage here the possible orientations of electrons with respect to centre of inner part of carbon atom known as nucleus while be in the phase of gas, graphite, fullerene, diamond, lonsdaleite and graphene where possible levity gravity behavior existing at electron level is drawn as well following by their Mohs hardness drawn on the basis of information available in the literature.

Experimental details:

To synthesize 'tiny grains carbon films', a technique known as MPE-CVD (IPLAS-Cyrannus, 2.45 GHz) was employed. A schematic of the MPE-CVD set up have been shown in previously published work [41]. Silicon wafers known in N-type nature resistivity $\sim 1-5$ (Ohm-cm) were used as the substrate material. Initial duration of the process (at nucleation stage) was set 30 minutes, whereas, deposition time (growth stage) was set 60 minutes in each experiment. Prior to loading the samples in the chamber, substrates were cleaned by ultrasonic agitation for the duration of 30 minutes in methanol solution containing nanodiamond powders size ~ 30 nm and titanium powders of 325 mesh for the purpose to create nucleation sites. The total mass flow rate was 200 sccm and was kept constant in each experiment. The substrate temperature was measured by K-type thermocouple where 6 % H_2 in argon –rich methane mixture was used to synthesize carbon films and the recorded

value was $700^{\circ}\text{C}\pm 10^{\circ}\text{C}$, whereas, the temperature was significantly lowered in films synthesized without H_2 where recorded value was $500^{\circ}\text{C}\pm 10^{\circ}\text{C}$. On increasing chamber pressure from 100 torr to 200 torr at constant microwave power 1400 (watts), no remarkable difference in temperature was noted. Due to lower thermal conductivity of Ar than H_2 heating of substrate by plasma is greatly reduced in Ar-rich CH_4 mixture [22]. Surface morphologies of 'tiny grains carbon films' were analyzed by Field Emission Scanning Microscope known as FE-SEM (ZEISS, Model: SIGMA). Peaks related to various phases were identified by Raman spectroscopy (Renishaw; 325 nm and HR800 UV; 632.8 nm). Photon field emission (PFE) characteristics known as electron field emission (or field electron emission) characteristics of 'tiny grains carbon films' were conducted by using a tunable parallel plate set-up known in $I-V$ curve and measurements were made by employing an electrometer (Keithley 237) under vacuum level of 10^{-6} torr. Dark field, bright field, high resolution images and selected area photon reflection (SAPR) patterns (known as SAED patterns) of various 'tiny grains carbon films' were taken by high resolution transmission microscope (known as HR-TEM, JEOL JEM2100F) operated at 200 kV. Energy of different bands in 'tiny grains carbon films' was deduced by core loss photon energy loss spectroscopy (core loss PELS) and low loss photon energy loss spectroscopy (low loss PELS) known as core loss EELS and low loss EELS, respectively.

Results and discussion:

Surface morphology of 'tiny grains carbon films' comprised various size and shape of tiny grains synthesized at different chamber pressures are shown in Figures S1 (a) to S1 (c); at 150 torr more tiny grains are in needle-like shapes. In carbon thin films synthesized at 100 torr and 200 torr, tiny grains are composed more in the shape of tiny clusters. Morphological features of tiny grains in film synthesized without H_2 gas (Figure S2) are almost identical to the ones in film synthesized at 6 % H_2 (Figure S1b). Raman spectra of different films synthesized at 100 torr, 150 torr and 200 torr are shown in Figure 1 indicating different intensity levels of peak related to ' ν_1 band'. The ' ν_1 band' in films synthesized at 100 torr and 200 torr is more pronounced as compared to the film synthesized at 150 torr. On the other hand, the ' ν_1 band' is intensive in film synthesized without H_2 gas (Figure S3) as compared to the films synthesized at 6% H_2 (Figure 1). In various Raman spectra, the peak related to ' ν_1 band' is at low level of intensity compared to D^* , D and G peaks. Field emission

current density (in known units) as a function of applied field (in known units) at various chamber pressures is shown in Figure 2. Film synthesized at 100 torr shows superior field emission properties where ‘turn on field’ is 11.52 V/ μm (the lowest value) and the large current density ($> 2.0 \text{ mA/cm}^2$). The ‘turn on field’ is the highest (25 V/ μm) in the film synthesized at 150 torr, whereas, it is recorded 16.4 V/ μm at 200 torr.

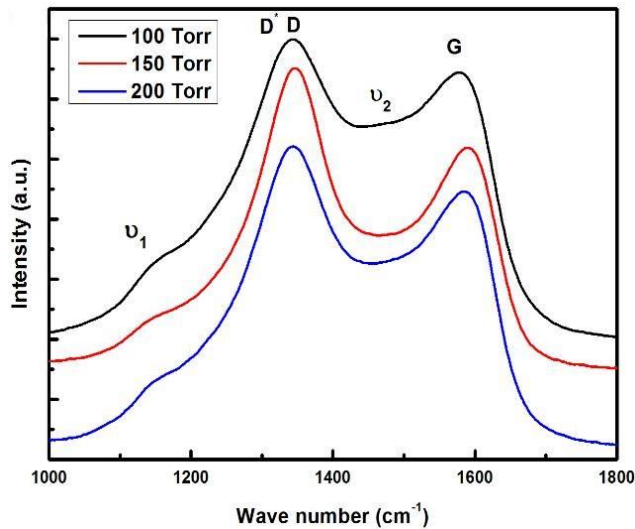


Figure 1: Raman spectra of ‘tiny grains carbon films’ synthesized at chamber pressure 100 torr, 150 torr and 200 torr; total mass flow rate: 200 sccm (6% H₂, 1 % CH₄ and 93 % argon, Ar: CH₄: H₂ = 186:2:12), microwave power: 1400 (in watts) and deposition time: 60 minutes.

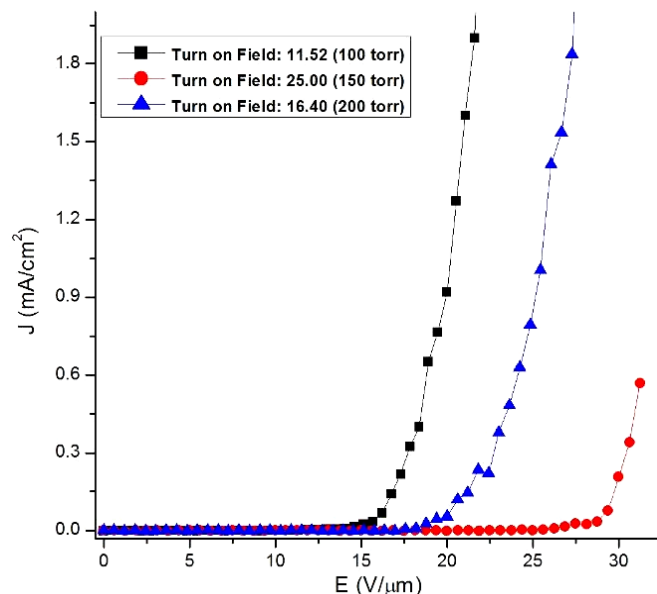


Figure 2: Field emission current density as a function of applied field of ‘tiny grains carbon films’ synthesized at chamber pressure 100 torr, 150 torr and 200 torr; total mass flow rate: 200 sccm (6% H₂, 1 % CH₄ and 93 % argon, Ar: CH₄: H₂ = 186:2:12), microwave power: 1400 (in watts) and deposition time: 60 minutes.

Field emission current density as a function of applied field in different 'tiny grains carbon films' synthesized without H₂ and with H₂ (3% and 6%) in Ar-rich CH₄ mixture are shown in Figures S4 (a-c). In Figures S4 (a) to S4 (c), the general trend of the 'turn on field' is more morphology-dependent; the value of 'turn on field' at 100 torr is lower than that at 150 torr (same trend in Figure 2). Under lower chamber pressure (at 100 torr), impingement of electron streams to 'graphitic phase tiny grains' appear to be highly effective, thus, more number of tiny grains modified into smooth elements as low 'turn on field' value was measured, whereas, the large value of 'turn on field' in film synthesized at 200 torr (Figure S4a) appeared to be due to less number of elongated 'graphitic phase tiny grains' of 'tiny grains carbon film'.

Dark field transmission microscope images of 'tiny grains carbon films' synthesized at 100 torr and 200 torr are shown in Figures S5 (a) and S6 (a) where small-sized dark spots are related to isolated tiny grains and bigger dark spots are related to coalesced (packed) tiny grains and contrast is more visible in bright field transmission microscope images shown in Figures S5 (b) and S6 (b); in some regions of the film, tiny grains amalgamated and in some regions of the film, tiny grains dispersed. SAPR patterns taken nearly in the same regions of films (shown in Figures S5b and S6b) are shown in Figures S5 (c) and S6 (c) where intensity spots don't show precise rings related to graphitic phase and the reflection (known as diffraction) pattern is more related to mixed behavior of structure. As indicated in the marked size of scale, which is nearly a half of the nanometer where photons reflected at the surface of structure (in both patterns) don't reveal any specific orientation of spotted intensities in related patterns.

High resolution transmission microscope image taken from 'tiny grains carbon film' synthesized at 100 torr is shown in Figure 3 (c) and from the figure, two regions of magnified images are shown in Figures 3 (a) and 3 (b). In Figure 3 (c), several tiny grains show their modification into smooth elements as they developed initially into graphitic phase –a two-dimensional structure termed as master structure. In the image, the most of regions reveal underlying tiny grains to appearable ones have also been modified into smooth elements. Such overlying behavior of 'modified graphitic phase tiny grains into smooth elements' is more pronounced in Figure 3 (a). In Figure 3 (b), a 'graphite structure tiny grain' modified into perfect smooth elements is shown. The insert in Figure 3 (c) shows spectral analysis of the modified structure

(shown in Figure 3b), which again reveals the smooth elements of ‘modified graphite structure tiny grain’.

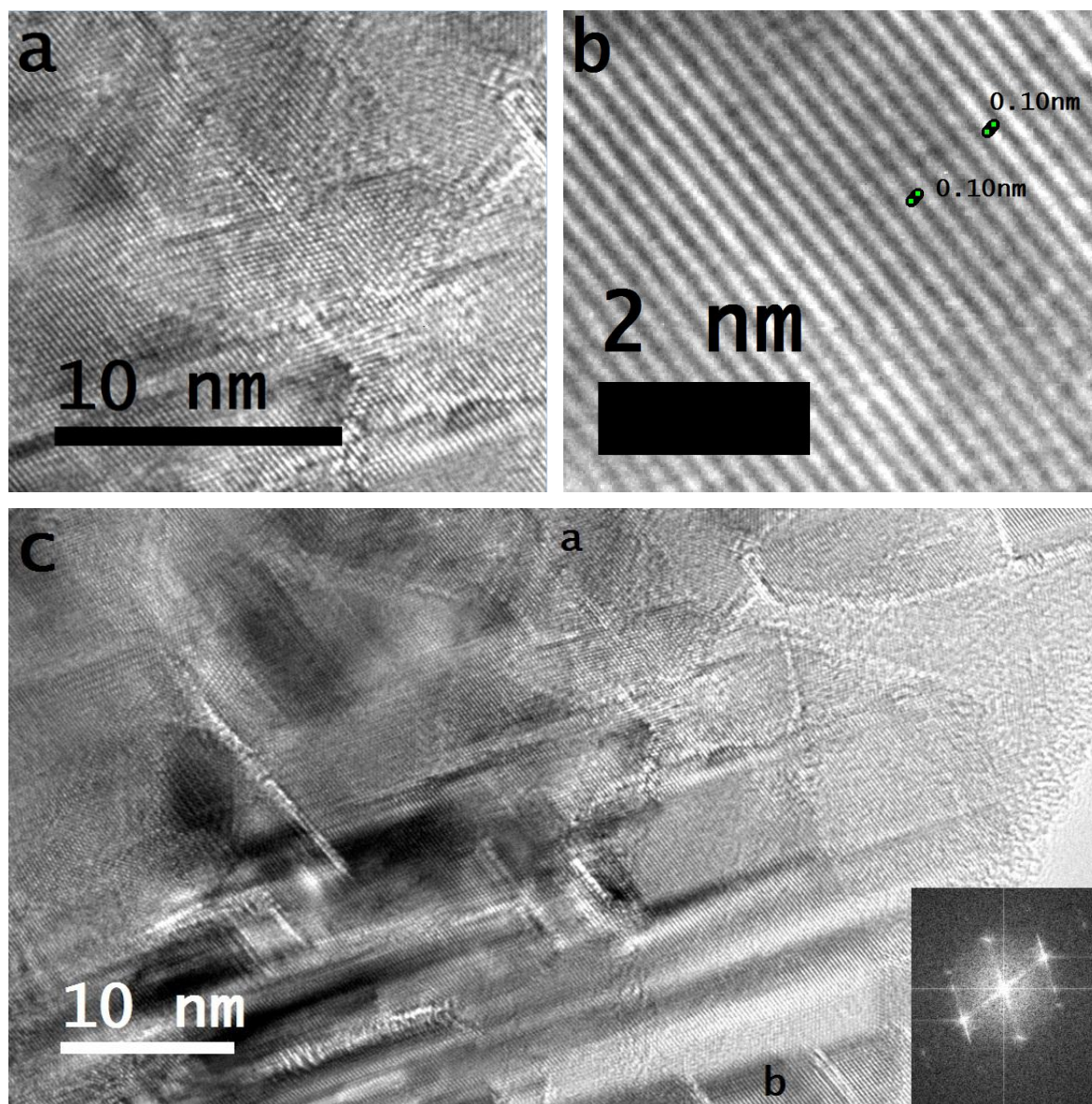


Figure 3: (a) Magnified view of the selected region of high resolution transmission microscope image shows several overlay ‘modified graphitic phase tiny grains’, (b) magnified view of the selected region of high resolution transmission microscope image shows ‘modified graphite structure tiny grain into smooth elements’ and (c) standard high resolution transmission microscope image shows large number of ‘graphitic phase tiny grains’ modified into smooth elements; ‘tiny grains carbon film’ synthesized at chamber pressure: 100 torr, mass flow rate: 200 sccm (6% H₂, 1 % CH₄ and 93 % argon), microwave power: 1400 (in watts) and deposition time: 60 minutes.

Figure S7 shows high resolution transmission microscope image taken from another region of the carbon thin film, which highlights different features of the tiny grains in carbon film. Gap between two grating like shapes labeled by (2) indicates formation of canal-like channel which is referred as ‘graphitic filament’ [39, 41]. High

resolution transmission microscope image taken from the carbon thin film synthesized at 200 torr is shown in Figure 4 (c) and from the figure, two regions of magnified high resolution transmission microscope images are shown in Figures 4 (a) and 4 (b). In Figure 4 (a), the tiny grains are in graphite structure (two-dimensional structure) but in Figure 4 (b) a tiny grain elongated and modified into smooth elements under the energy of travelling hard X-rays photons. A canal-like channel is formed between two tiny grains denoted by red dotted line in Figure 4 (b) where they modified into smooth elements. The insert in Figure 4 (c) shows spectral analysis of 'graphite structure tiny grain' (which didn't elongate and modify as shown in Figure 4a) where intensity spots spotted by (energy intensity of) reflected photons at the surface also reveal two-dimensional structure, which is not the case of insert image in Figure 3 (c) as it reveals formation of smooth elements.

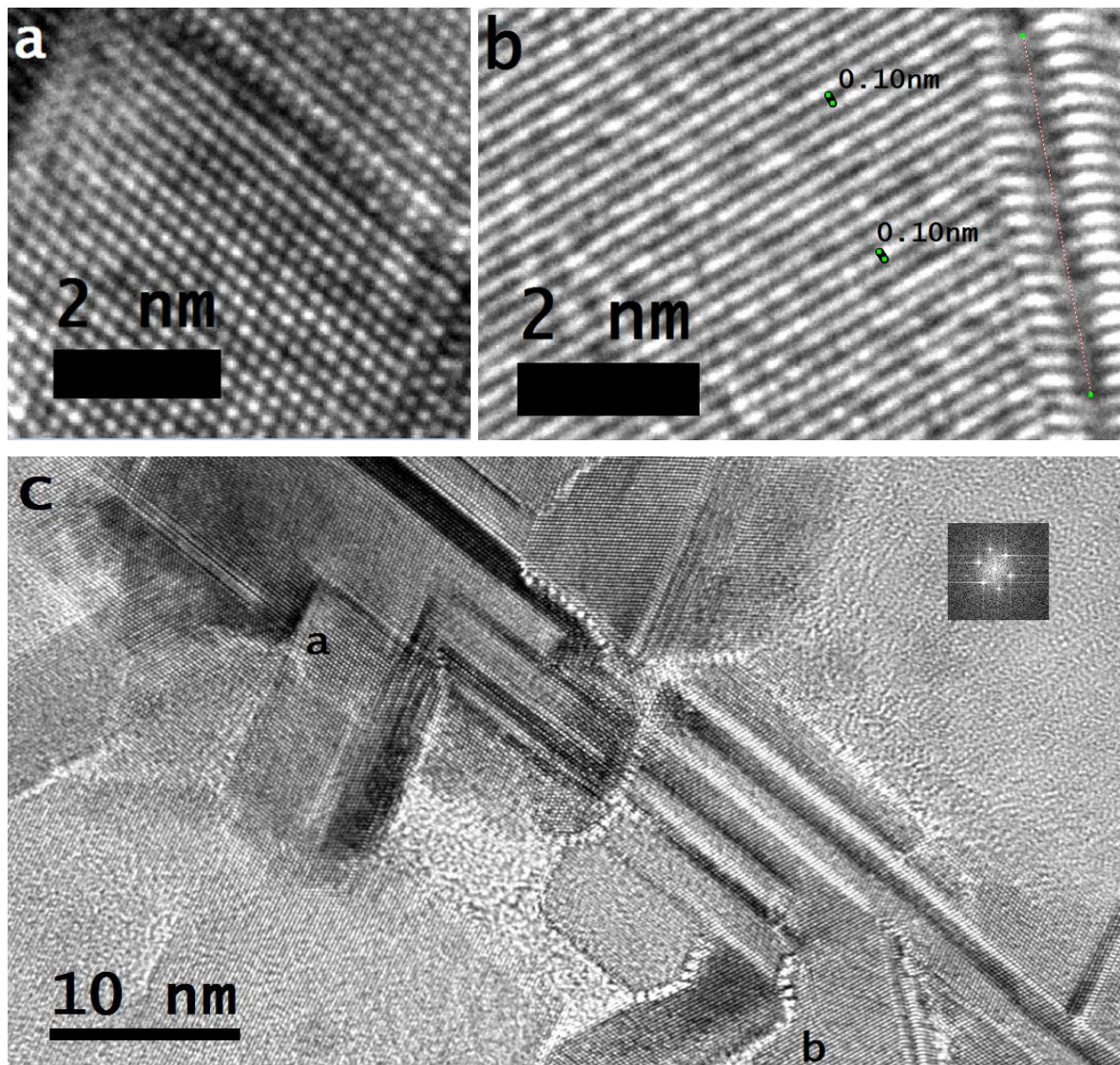


Figure 4: (a) Magnified view of the selected region of high resolution transmission microscope image shows 'graphitic phase tiny grain', (b) magnified view of the selected region of high resolution transmission microscope image shows 'modified graphite structure tiny grain into smooth elements' and (c) standard high resolution transmission microscope image shows several tiny grains where some retained graphite structure and some modified into smooth elements (insert shows spectral analysis of region 'a'); 'tiny grains carbon film' synthesized at chamber pressure: 200 torr, mass flow rate: 200 sccm (6% H₂, 1 % CH₄ and 93 % argon), microwave power: 1400 (in watts) and deposition time: 60 minutes.

From these high resolution microscopy images, it is not possible to identify those phases of carbon known in their exceptional hardness as the orientational positions of electrons with respect to center of inner part of atom known as nucleus is too small in each case. However, it is essay to point out the elongation behavior of atoms (modification of tiny grains into smooth elements) and deformation behavior as well. Here, 'electronic structure' is referred to that structure where electron states of atoms stretch, orientationally or non-orientationally, thus, referred those atoms as 'elongated atoms' and in the case of elongation of 'graphitic phase tiny grain' it is referred to 'elongated tiny grain', such structure modify into smooth elements as while travelling photons of hard X-rays where their energy wavelength perfectly suited to align those elongated tiny grains into smooth elements. In such 'carbon tiny grains films' where propagation of photonic current is accelerated and because of that, they are famous in the enhanced field emission applications where inter-state electron's gap becomes stable, non-stop and straight, thus, allow propagation of accelerated current density of photons wavelength in inter-state electron's gap. In the elongated 'graphitic phase tiny grains' travelling photons of hard X-rays photons modify them into smooth elements which have the same width as well as inter-spacing distance (gap) between two smooth elements as shown in Figures 3 (b) and 4 (b). This clearly reveals that a tiny-sized particle or quantum dots (or the larger ones) evolve two-dimensional structure doesn't collectively oscillate on trapping or coupling light (photons) and photons of adequate wavelength enable their modification into smooth elements when elongated uniformly.

Core loss PELS obtained at the same region of 'tiny grains carbon films' from where high resolution transmission microscope images were taken as shown in Figures 5 (a) and (b). An abrupt rise near 292 eV referred to σ^* -band and a large dip in the vicinity of 305 eV referred to diamond phase [42, 43] and these bands are also found in the films synthesized at 100 torr and 200 torr as shown in Figures 5 (a) and

(b). However, in our opinion the large dip curve in both films, which is more indicative in the case film synthesized at 200 torr (Figure 5b), is due to energy of band related to tiny grains modified into smooth elements (~ 285 eV). The core loss PELS of both films reveal the same energy peaks related to different bands and identical trend to the one observed in the case of Raman spectroscopy. But in the case of Raman spectroscopy, the peaks' positions were at different wave number, whereas, in core loss PELS the peaks' positions are at different band; tiny grains of carbon films modified into lonsdaleite, diamond and graphene phase are at peak ~ 295 (eV), ~ 308 (eV) and ~ 328 (eV), respectively. Tiny grains of carbon films remained in graphitic phase reveal decreasing level of energy in the form of dip curve at band ~ 304 (eV) in both films as notable in Figures 5 (a) and (b). In Figures 5 (a), more pronounced hump-like peaks at ~ 328 eV is due to more tiny grains of carbon films modified into graphene phase.

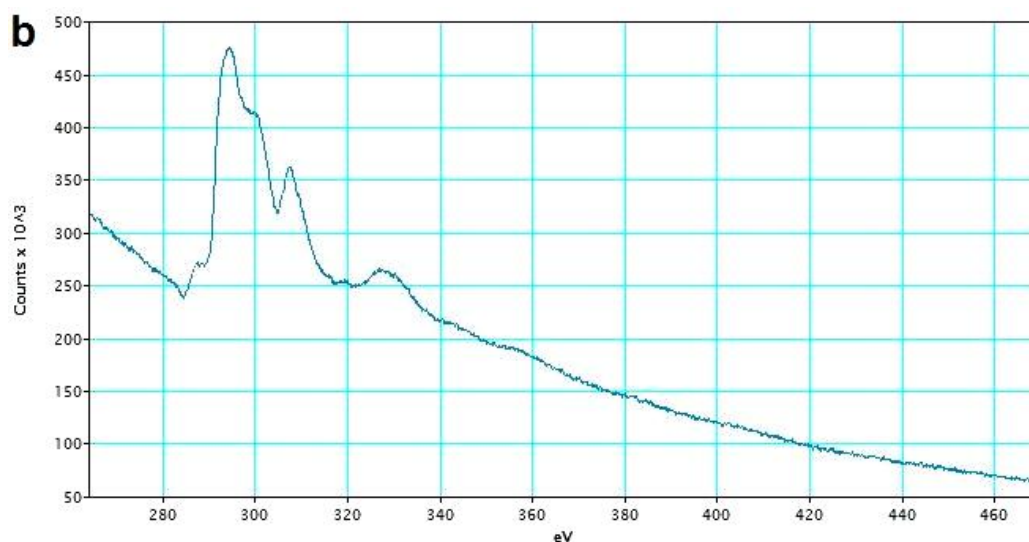
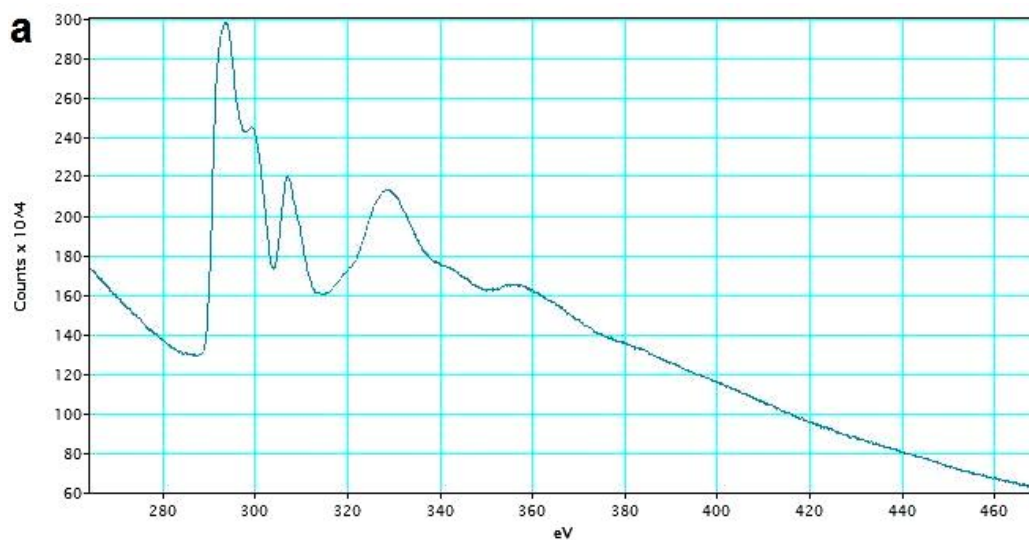


Figure 5: Core Loss photon energy loss spectroscopy (known as core loss EELS) of ‘tiny grains carbon films’ synthesized at chamber pressure (a) 100 torr and (b) 200 torr; total mass flow rate: 200 sccm (6% H₂, 1 % CH₄ and 93 % argon), microwave power: 1400 (watts) and deposition time: 60 minutes.

In low loss EELS, graphitic phase shows a prominent peak at s₃ (27 eV), whereas, the a-C phase shows a peak at s₁ (22 eV) [43, 44]. However, in low loss PEELS shown in Figures 6 (a) and (b), a peak at 27 eV is not available and also band is at slightly tilted position instead of at 22 eV for both ‘tiny grains carbon films’ indicating different trend of phase transitions of tiny grains and also different trend within these films. Overall, the trend of peaks’ behavior related to different band energy is in the same manner as observed in the case of core loss PEELS of these films. The built-in unit (eV) in the case of core loss PEELS and low loss PEELS can be replaced with photon volts (pV).

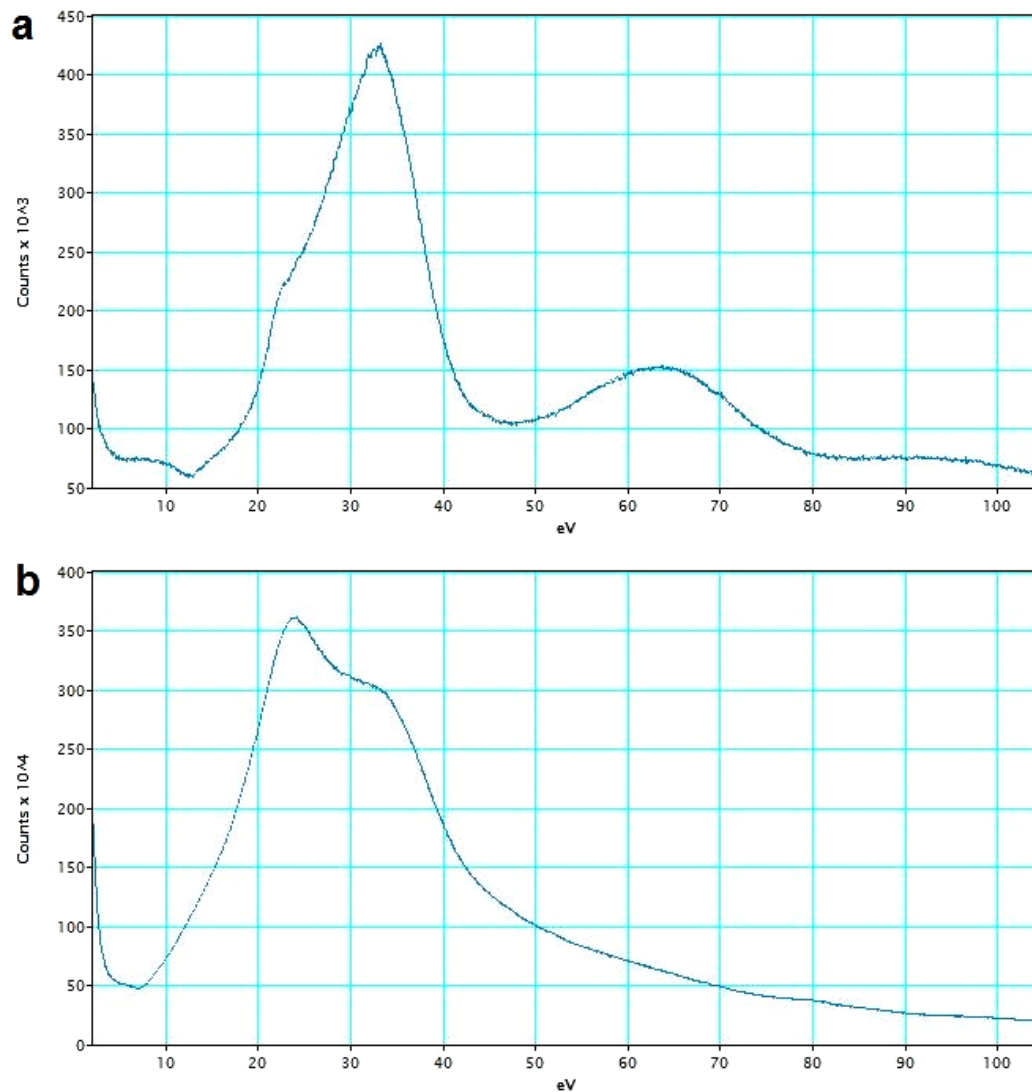


Figure 6: Low loss photon energy loss spectroscopy (known as low loss EELS) of ‘tiny grains carbon films’ synthesized at chamber pressure (a) 100 torr and (b) 200 torr; total mass flow rate: 200 sccm (6% H₂, 1 % CH₄ and 93 % argon), microwave power: 1400 (watts) and deposition time: 60 minutes.

In Raman spectra of NCD/UNCD films, the peak at 1150 cm⁻¹ has been attributed to nanocrystalline diamond [44-46], however, the ν_1 peak (at 1150 cm⁻¹) cannot originate from a nanodiamond or related sp³-bonded phase but assigned to transpolyacetylene segments at grain boundaries and surfaces [47]. Nemanich *et al.* [45, 46] proposed that 1150 cm⁻¹ peak arises from nanocrystalline or amorphous diamond. In the Raman spectrum of NCD/UNCD film, the sharp peak at 1332.1 cm⁻¹ is the characteristic of diamond and broadening of the peak is related to the NCD grains [48]. In NCD/UNCD films, the peak at 1150 cm⁻¹ appears hypothetically due to CH bonds and is always linked to another peak at 1450 cm⁻¹, and the peaks at 1330 cm⁻¹ and 1560 cm⁻¹ are due to D-band and G-band [49]. However, in the light of presented results of ‘tiny grains carbon films’, argon gas increased the rate of re-nucleation and the amount of tiny grains sizes < 10 nm enhanced significantly. Depending on how many ‘graphitic phase tiny grains’ modified into smooth elements, their quantity experienced Raman laser recorded the contribution in the form of peak at wave number ~ 1150 cm⁻¹. In microcrystalline diamond films, the size of grains is very large at large extent where they switch to another phase due to varying localized conditions [1], thus, don’t retain graphitic phase and mainly modified into diamond phase at large extent while coordinating to large amount of made atomic hydrogen in HFCVD, accordingly, information put forth by Raman signals rather to record peak at 1150 cm⁻¹, the peak is recorded at 1332 cm⁻¹. Thus, the peak at wave number 1150 cm⁻¹ is associated to those tiny grains developed in their graphitic phase followed by their modification into smooth elements and depending on the amount of ‘modified graphitic phase tiny grains into smooth elements’ the intensity of ‘ ν_1 peak’ is varied; different intensity of ‘ ν_1 band’ is related to the number of the tiny grains modified into smooth elements under the Raman laser. Those tiny grains of graphite structure didn’t elongate but retained two-dimensional structure which becomes the origin of ‘ ν_2 peak’ in the Raman spectrum. In this way wherever the ‘ ν_1 peak’ is resulted in the Raman spectrum of carbon films the ‘ ν_2 peak’ is resulted as well. Incorporating H₂ in Ar-rich CH₄ mixture either eliminates the ‘ ν_1 band’ or it appears with less intensity. Without incorporation of H₂ in Ar-rich CH₄ mixture, peak

related to ' ν_1 band' is become pronounced as shown in Figure S3. On varying concentration of feed gases, the nature of tiny grains is varied as well, thus, counting different numbers of 'modified graphitic phase tiny grains into smooth elements', which record different intensity of ' ν_1 band' in the Raman spectrum. Again, different intensity of ' ν_1 band' is recorded on dealing Raman signals of different wavelength [50, 51], which is due to dealing varied levels of energy by 'modified graphitic phase tiny grains into smooth elements' in the same carbon film.

In Raman spectroscopy, the peaks at different wave numbers are resulted because of propagating energy of interacting Raman laser in a different manner owing to different phases of tiny grains in a carbon film as shown in Table 1; at wave number $\sim 1145 \text{ cm}^{-1}$, the peak (due to ν_1 band) is related to 'modified graphitic phase tiny grains into smooth elements' is resulted and at wave number $\sim 1310 \text{ cm}^{-1}$, the peak (due to D^* band) related to 'tiny grains modified into lonsdaleite phase' is resulted, and at wave number $\sim 1332 \text{ cm}^{-1}$, the peak (due to D band) related to 'tiny grains modified into diamond phase' is resulted, and at wave number $\sim 1480 \text{ cm}^{-1}$, the peak (due to ν_2 band) related to 'tiny grains retained graphitic phase' is resulted and finally, at wave number $\sim 1580 \text{ cm}^{-1}$, the peak (due to G band) related to 'tiny grains modified into graphene phase' is resulted. Where carbon atoms/their tiny grains remain in amorphous structure, small peaks are also being originated in the Raman spectrum between 1350 cm^{-1} to 1550 cm^{-1} . In Table 1, wavelength of resulted Raman peaks related to different phases is decreasing at increasing wave number indicating increase in the frequency under decreasing wavelength. In the case of ' ν_1 peak', the lowest energy of the structure resulted for 'modified graphitic phase tiny grains into smooth elements' in the form of dip curve at ~ 285 (measured in eV) at core loss PEELS, thus, gives the longest recorded wavelength ($\sim 8734 \text{ nm}$) in the Raman spectrum. On the other hand, where tiny grains modified into graphene phase, the highest energy of the phase resulted (~ 328 measured in eV) at core loss PEELS, thus, gives the shortest wavelength in the Raman spectrum ($\sim 6329 \text{ nm}$). Therefore, tiny grains work under the lowest energy of the phase and the longest wavelength (shortest wave number) result into propagate photonic current at high acceleration as in the case of 'modified graphitic phase tiny grains into smooth elements', thus, their greater amount available in a carbon film results into enhance the field emission characteristics.

As tabulated in the Table 1 that ‘modified graphitic phase tiny grains into smooth elements’ give the highest value of wavelength indicating that they are the cause of enhanced field per unit length or area as discussed in the case of field emission characteristics of ‘tiny grains carbon films’. In the case of lonsdaleite, diamond and graphene phases, the decreased values of wavelength are resulted under the certain selection of rule set by designated orientation of sets of electrons of their atoms known in exhibiting unprecedented hardness. Now the question arises that recorded wavelength in the case of graphite structure is also between diamond and graphene (in Table 1) but measured hardness is at very low level, however, the peak related to graphitic phase is at very low intensity in the Raman spectrum and also we can observe that energy related to graphitic phase is in the form of dip curve in the spectrum of photon energy loss spectroscopy. The scheme of electrons is different in graphitic phase and modified phases, thus, delivered different response of the coordinated or interacted signals, which is distinctive in graphitic phase due to neutral behavior of levity gravity of sets of electrons of their atoms. Despite the fact, input energy entering to ‘tiny grains carbon films’ was the same for graphitic phase and different modified phases but the resulting outcome varied as per inter-state electron’s gap becoming viable of atoms made in the case of different phases. These findings solicit to devise science of Raman spectroscopy and energy loss spectroscopy, accordingly.

Table 1: Tiny grains of carbon films reveal Raman peaks at varying wave number (1/wavelength) and energy peaks at varying band when retained graphitic phase (master structure) and when modified graphitic phase into smooth elements and into other natural sorts of modifications

Modified graphitic phase tiny grains into smooth elements; more as an artificial phase	Lonsdaleite (a modified phase); ; more as a natural phase	Diamond (a modified phase); more as a natural phase	Graphite structure (master structure)	Graphene (a modified phase); more as a natural phase
Raman spectroscopy (in cm⁻¹)				
$\nu_1 \sim 1145$ (8734 nm)	D* ~ 1310 (7634 nm)	D ~ 1332 (7508 nm)	$\nu_2 \sim 1480$ (6757 nm)	G ~ 1580 (6329 nm)
Core loss photon energy loss spectroscopy (in eV)				
Dip curve at ~ 285	Peak at ~ 295	Peak at ~ 308	Dip at ~ 304	Peak at ~ 328

In MPE-CVD process, carbon atoms dissociated from the precursor at different rates resulting into attain different dynamics along with localized heating through which atomic bindings take place. In such cases, an atom can bounce back due to non-executing concurrent electron-dynamics at the instant of its amalgamation and the new comer may bind under different orientation of its executed electron-dynamics resulting into the evolution of amorphous structure. In the case of attaining uniform dynamics of atoms along with chasing the execution of concurrent electron-dynamics results into two-dimensional structure of tiny grain, which is graphite structure, also termed as master structure. As argon atoms split under the field of photonic current in MPE-CVD system and electrons streams impinge such tiny grains at fixed angle, it results into their elongation as discussed in the case of gold tiny particles [4, 10], silver and binary composition of gold/silver [6] and also in the case of single atom embedded in tiny-sized particle [11]. Argon atoms, on splitting, shoot their electron streams to underlying matter where comprised atoms possess the feature to stretch electrons' states as per available room. Such tiny grains are said to be 'elongated tiny grains' and they deal modification into smooth elements while placing or travelling photons of hard X-rays to their surface of monolayer structure. Those elongated tiny grains modified electronic structure into smooth elements under the energy of travelling photons of hard X-rays, which are available in the chamber in plentiful and viable for the job, that is, converting elongated tiny grains into smooth elements, thus, they are termed as 'modified graphitic phase tiny grains into smooth elements' in Table 1.

Again, presence of atomic hydrogen as well as oxygen in the chamber where carbon atoms (when in solid state) in many tiny grains while evolving master structure gravitize sets of electrons under the fixed orientation of electron-electron coordination *via* unfilled states available in their outer states resulting into modify structure to various carbon phases known in their exceptional hardness. Atomic hydrogen and atomic oxygen only facilitate to sets of electrons of carbon atoms to tack at a particular orientation with respect to centre of inner part of atom known as nucleus. Such modified phases of carbon atoms where sets of electrons have been tacked at certain orientation with respect to centre of inner part of atom deal natural sorts of modifications instead of elongating and while travelling hard X-rays photons modifying into smooth elements.

Despite nano-twinned microstructures diamond size, extraordinary hardness and thermal stability was measured [52] indicating the dealing of diamond phase of each tiny grain following by each atom. However, UNCD/NCD film synthesized by process other than MPE-CVD and HF-CVED reveals the elongated tiny grains of carbon films as well, as they made smooth elements [53].

Owing to neutral behavior of levity gravity, a carbon atom reveals graphitic phase where both sets of electrons are at ground state, in the presence of atomic hydrogen or atomic oxygen (or both) in certain environment results into modification of graphitic phase of carbon atom into diamond phase or graphene phase. The underpinning mechanism of carbon atom while in gaseous phase is shown in Figure 7 (a) where only levity prevailed by keeping tacking both sets of electrons' position toward North as long as levitational force is remained intact. A carbon atom remains in graphitic phase as long as reveal neutral (equal level) levity gravity in both sets of electrons as shown in Figure 7 (b). A carbon atom is in fullerene phase (buckyballs and carbon nanotubes) or in other closely-related phases (morphology of carbon films is more like shape of flake, needle, flower, etc.) as long as rotating and exchanging the prevailed behaviors of less levity and more gravity at $\sim 5^\circ$ angle to $\sim 40^\circ$ in each set of electrons residing nearly opposite sides of the nucleus as shown in Figure 7 (c). Carbon atom is in diamond phase when both sets of electrons reveal gravitation behavior while maintaining distance between them as shown in Figure 7 (d) where feasibility of their forming angle is at $\sim 109^\circ$ with respect to centre of nucleus, which is due to gravitization through atomic hydrogen. Carbon atom is in lonsdaleite phase when both sets of electrons reveal gravitation behavior while maintaining distance between as shown in Figure 7 (e) where feasibility of their forming angle is at $\sim 60^\circ$ with respect to centre of nucleus, which is under greater extent gravitization of sets of electrons through atomic hydrogen. Carbon atom is in graphene phase when both sets of electrons reveal gravitation behavior (South-pole) while maintaining nearly zero inter-distance as shown in Figure 7 (f), which is due to gravitization of sets of electrons though atomic oxygen. Carbon atoms where they reveal different sorts of electrons' orientation other than shown in Figure 7 (a-f) evolve amorphous structure. The sketch of atom for each carbon atom phase in Figure 7 is the estimated one where nucleus also includes particles termed as protons, obviously, their layout cannot be like as for

particles termed as neutrons and will be discussed in a separate submission how to deal particles known in their positive charge.

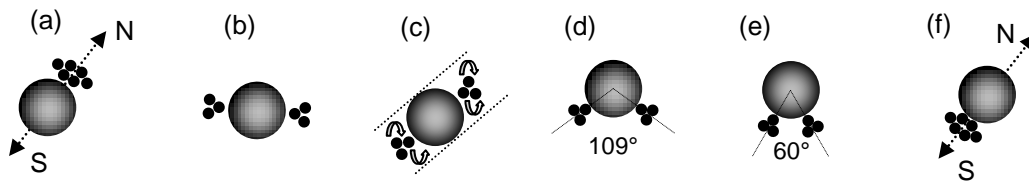


Figure 7: Carbon atom in (a) gaseous phase, (b) graphitic phase, (c) fullerene phase or other closely-related phases, (d) diamond phase, (e) lonsdaleite phase and (f) graphene phase.

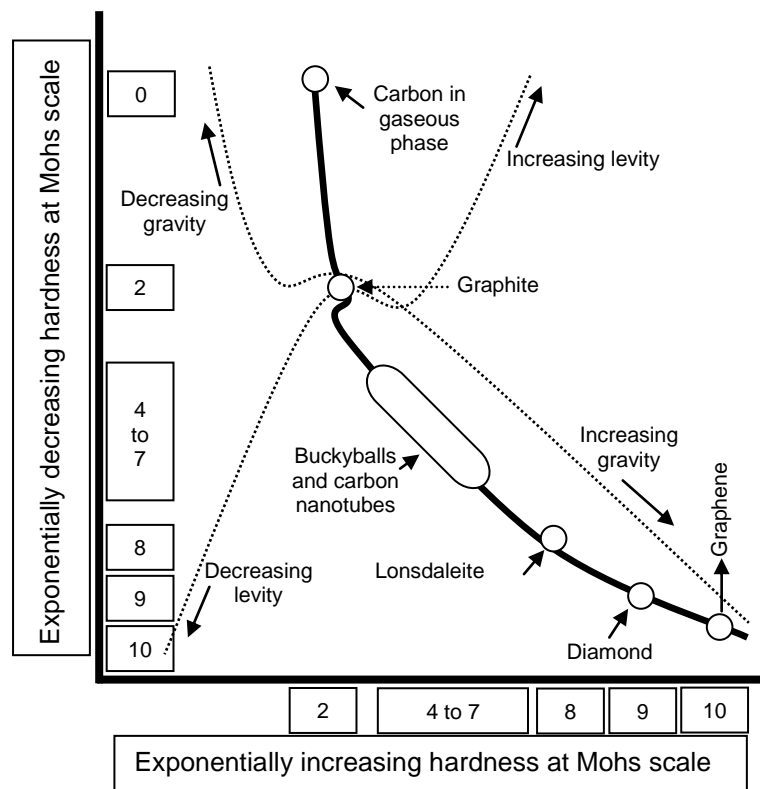


Figure 8: A sketch of approx. hardness (at Mohs scale) of graphitic phase along with various modified phases versus levitation gravitation behavior.

As the carbon atoms are in their different phases, in a gaseous phase and in several phases of solid phase where a graphitic phase is an original (master) phase and other are the modified ones; fullerene, diamond, lonsdaleite and graphene. Master structure of carbon also modified into smooth elements as discussed above. Hardness at Mohs scale of carbon atoms while dealing graphitic phase and different modified phases at nanoscale is sketched in Figure 8. Zero value of hardness accounts in the case of carbon in gaseous state. The hardness of graphitic phase and various modified phases are related to originally built-in behavior of levitation field or gravitation field or mixed/neutral behavior of sets of electrons around the

nucleus of carbon atoms. Different value of wave number of printed (recorded) energy signals (photons) from graphitic phase and modified carbon phases in Raman spectroscopy which means different gaps/approach of propagating photons of electron states as verified by the peaks related to each phase in energy loss spectroscopy. The drawn graph in Figure 8 reveals trend of hardness on the basis of energy related to each carbon phase. Carbon atoms have the option to tack sets of electrons at certain positions around the nucleus and all are the stabilized phases. Electron states in H and O atoms are suitable in achieving the gravitized behavior to certain extent of both sets of electrons in carbon atoms. A diamond phase of carbon atoms never goes to corroded (oxidized state) as the electrons have been shifted at downside to nucleus forming angle of each set of electrons 109° with respect to centre of nucleus and same is the case when water gravitized converting into solid ice where same degree angle of each set of electrons with respect to centre of nucleus is expected. Slippery graphite is not due to the presences of weak forces but due to neutral behavior of levity gravity of electrons of carbon atoms.

Our experimental studies show nearly the same width of each made smooth element along with inter-spacing distance of smooth elements in gold and silver [4-8] as in the case of carbon (in Figures 3 and 4). Thus, it can be inferred that the size of each electron in the case of carbon is much bigger to what an atom owes in the case of gold or silver. This is the reason that materials based on carbon deal a very high temperature in their measurements, which is again much more than what recorded in the case of gold (or silver) well justifying the different size of their electrons. Again, the requirement of heat energy (temperature) is also in the same limit when synthesizing carbon-based materials in techniques known as hot filament chemical vapor deposition, microwave plasma chemical vapor deposition, etc. In this context, the requirement of shut energy to enable to free the electron at target should enhance significantly as compared to the one in silicon or in other suitable atoms of solid state behavior.

Either formation of tiny grains prior to deposit (stick) at substrate or on depositing the atoms at substrate, one by one, later made the tiny grains, in both cases, participated carbon atoms have been achieved their solid state behavior (from gaseous state), under the process of synergy, and at first hand, atoms will made two-dimensional structure as they attain electron-dynamics under neutral behavior of levity gravity, this is why, it has been said that graphitic phase is a master structure

where atoms are in their two-dimensional order. But, due to one or more reasons, and where atoms don't bind in their two-dimensional order, an amorphous structure grows. However, graphitic phase is the cause of all sorts of more like artificial modifications ((where electron states of atoms stretch orientationally (atoms elongate) or non-orientationally (atoms deform)) and more like natural modifications (where electron states of atoms neither stretch orientationally nor non-orientationally but tack at particular orientation at the surface of surface of atom with respect to inner center known as nucleus.

Conclusions:

'Tiny grains carbon films' synthesized under different conditions of the pressure and amounts of hydrogen where carbon atoms amalgamated on highly smooth prepared seeded surface of silicon wafers under attained dynamics, on binding atoms under electron-dynamics while heating locally resulting into evolve a master structure, namely, graphite structure (two-dimensional structure) or a amorphous structure under uniform photon couplings or non-uniform photon couplings, respectively. Tiny grains adopt master structure where all atoms instate solid state behavior as long as dealing same attained dynamics and uniform electron-dynamics. Tiny grains evolved in two-dimensional structure elongate following by modification of made electronic structure into smooth elements while travelling photons of hard X-rays. 'Modified graphitic phase tiny grains into smooth elements' of a carbon film are the origin of ν_1 peak in the Raman spectrum and reveal the lowest wave number where enhanced field emission performance is resulted under accelerated and improved current density rate, whereas, tiny grains retain graphitic phase are the origin of ν_2 peak and field emission characteristics of various known NCD/UNCD films are largely dependable on the ratio of those peaks.

Overall, in low loss photon energy loss spectroscopy, a same trend of various energy bands is observed as in the case of core loss photon energy loss spectroscopy. Results of field emission measurements of films synthesized at different pressure are in good agreement to energy loss spectroscopy and Raman spectroscopy along with morphology-structure. In Raman spectra, peaks related to D* band and G band are due to printed (recorded) energy signals propagated through modified inter-state electron's gap of atoms of tiny grains known in lonsdaleite and graphene, respectively. In energy loss spectroscopy, the peak

related to 'modified graphitic phase tiny grains into smooth elements' and 'graphitic phase' is in the form of dip curve due to lower band energy as compared to the ones modified into diamond, lonsdaleite and graphene phases. The wave number (inverse of wavelength) related to graphitic phase and 'modified graphitic phase tiny grains into smooth elements' in a carbon film, in fact, reveal inter-state's electron gap through which expedite rate of propagation of photons characteristics current are resulted, which is the highest in terms of wavelength in the case of 'modified graphitic phase tiny grains into smooth elements', thus, validates that enhanced field emission performance of a carbon film is related to higher amount of made smooth elements of tiny grains.

Under changing positions of sets of electrons around the nucleus switching phase of a carbon atom from one allotropic form to another where attained positions of electrons remained intact via field force acting from a distance under the conserved energy of an atom. In 'modified graphitic phase tiny grains into smooth elements', where stretching of electron states is orientation based, graphitic phase atoms elongate, so their tiny grains. However, in the case of modification of 'graphitic phase tiny grains', instead of stretching of electron states the positions of electrons in the form of sets are gravitized with respect to center of nucleus while coordinating accelerated atomic hydrogen, which results into either diamond phase or lonsdaleite phase depending on the angle between sets of electrons. A graphene phase is resulted when atomic oxygen coordinated to vacant electron states of atom.

Our experimental results well prove and justify the position of peaks related to graphitic phase and various modified phases both in terms of wavelength and band energy along with field emission characteristics. In line with this, present studies set a new horizon in synthesizing, analyzing and evaluating materials at nanoscale, and soliciting reinvestigation of materials' syntheses and their performances both for existing and future applications.

Acknowledgements:

Mubarak Ali thanks National Science Council (now MOST) Taiwan (R.O.C.) for awarding postdoctorship: NSC-102-2811-M-032-008 (2013-2014). Authors wish to thank Mr. Tsung-Min Chen for assisting films' synthesis and Mr. Chien-Jui Yeh in TEM operation. Mubarak Ali greatly appreciates useful suggestions of Dr. M. Ashraf Atta and Dr. Abdul Waheed (CIIT, advisors).

References:

- [1] M. Ali, M. Ürgen, Switching dynamics of morphology-structure in chemically deposited carbon films-a new insight, <http://arxiv.org/abs/1605.00943> (2016).
- [2] S. Link, M. A. El-Sayed, Shape and size dependence of radiative, nonradiative and photothermal properties of gold nanocrystals, *Int. Rev. Phys. Chem.* 19 (2000) 409- 453.
- [3] S. C. Glotzer, M. J. Solomon, Anisotropy of building blocks and their assembly into complex structures, *Nature Mater.* 6 (2007) 557-562.
- [4] M. Ali, I –N. Lin, The effect of the Electronic Structure, Phase Transition and Localized Dynamics of Atoms in the formation of Tiny Particles of Gold, <http://arXiv.org/abs/1604.07144> (2016).
- [5] M. Ali, I –N. Lin, Development of gold particles at varying precursor concentration, <http://arxiv.org/abs/1604.07508> (2016).
- [6] M. Ali, I –N. Lin, Tapping opportunity of tiny shaped particles and role of precursor in developing shaped particles, <http://arxiv.org/abs/1605.02296> (2016).
- [7] M. Ali, I –N. Lin, Controlling morphology-structure of particles at different pulse rate, polarity and effect of photons on structure, <http://arxiv.org/abs/1605.04408> (2016).
- [8] M. Ali, I –N. Lin, Formation of tiny particles and their extended shapes – origin of physics and chemistry of materials, <http://arxiv.org/abs/1605.09123> (2016).
- [9] M. Ali, Structure evolution in atoms of solid state dealing electron transitions. <http://arxiv.org/abs/1611.01255> (2016).
- [10] M. Ali, The study of tiny shaped particle dealing localized gravity at solution surface. <http://arxiv.org/abs/1609.08047> (2016).
- [11] M. Ali, Atoms of electronic transition deform or elongate but do not ionize while inert gas atoms split. <http://arxiv.org/abs/1611.05392> (2016).
- [12] M. Ali, Revealing the Phenomena of Heat and Photon Energy on Dealing Matter at Atomic level. *Preprints* (2017). <https://www.preprints.org/manuscript/201701.0028/>.
- [13] M. Ali, Why some atoms are in gaseous state and some in solid state but carbon work on either side (2017). (Submitted for consideration)
- [14] M. Ali, Nanoparticles –Photons: Effective or Defective Nanomedicine. *Preprints* (2017). <http://www.preprints.org/manuscript/201703.0174/v1>

- [15] W. Zhu, G. P. Kochanski, S. Jin, Low-Field Electron Emission from Undoped Nanostructured Diamond, *Science* 282 (1998) 1471-1473.
- [16] J. Birrell, J. A. Carlisle, O. Auciello, D. M. Gruen, J. M. Gibson, Morphology and electronic structure in nitrogen-doped ultrananocrystalline diamond, *Appl. Phys. Lett.* 81 (2002) 2235-2237.
- [17] J. E. Dahl, S. G. Liu, R. M. K. Carlson, Isolation and Structure of Higher Diamondoids, Nanometer-Sized Diamond Molecules, *Science* 299 (2003) 96-99.
- [18] J. Y. Raty, G. Galli, Ultradispersity of diamond at the nanoscale, *Nature Mater.* 2 (2003) 792-795.
- [19] S. C. Tjong, H. Chen, Nanocrystalline materials and coatings, *Mater. Sci. Engineer. R* 45 (2004) 1-88.
- [20] A. V. Sumant *et al.*, Towards the Ultimate Tribological Interface: Surface Chemistry and Nanotribology of Ultrananocrystalline Diamond, *Adv. Mater.* 17 (2005) 1039-1045.
- [21] A. R. Krauss, O. Auciello, M. Q. Ding, D. M. Gruen, Y. Huang, V. V. Zhirnov, E. I. Givargizov, A. Breskin, R. Chechen, E. Shefer, V. Konov, S. Pimenov, A. Karabutov, A. Rakhimov, N. Suetin, Electron field emission for ultrananocrystalline diamond films, *J. Appl. Phys.* 89 (2001) 2958-2967.
- [22] X. Xiao, J. Birrell, J. E. Gerbi, O. Auciello, J. A. Carlisle, Low temperature growth of ultrananocrystalline diamond, *J. Appl. Phys.* 96 (2004) 2232-2239.
- [23] O. A. Williams, M. Nesladek, M. Daenen, S. Michaelcon, A. Hoffman, E. Osawa, K. Haenen, R. B. Jackman, Growth, electronic properties and applications of nanodiamond, *Diam. Relat. Mater.* 17 (2008) 1080-1088.
- [24] A. R. Konicek, D. S. Grierson, P. U. P. A. Gilbert, W. G. Sawyer, A. V. Sumant, R. W. Carpick, Origin of Ultralow Friction and Wear in Ultrananocrystalline Diamond, *Phys. Rev. Lett.* 100 (2008) 235502-04.
- [25] J. E. Butler, A. V. Sumant, The CVD of Nanodiamond Materials, *Chem. Vap. Deposition* 14 (2008) 145-160.
- [26] J. P. Thomas, H. C. Chen, N. H. Tai, I -N. Lin, Freestanding Ultrananocrystalline Diamond Films with Homo Junction Insulating Layer on Conducting Layer and Their High Electron Field Emission Properties, *ACS Appl Mater Interfaces* 3 (2011) 4007-4013.

- [27] W. Kulisch, C. Petkov, E. Petkov, C. Popov, P. N. Gibson, M. Veres, R. Merz, B. Merz, J. P. Reithmaier, Low temperature growth of nanocrystalline and ultrananocrystalline diamond films: A comparison, *Phys. Status Solidi A* 209 (2012) 1664-1674.
- [28] K. J. Sankaran *et al.*, Improvement in plasma illumination properties of ultrananocrystalline diamond films by grain boundary engineering, *J. Appl. Phys.* 114 (2013) 054304-11.
- [29] K. J. Sankaran *et al.*, Improvement in Tribological Properties by Modification of Grain Boundary and Microstructure of Ultrananocrystalline Diamond Films, *ACS Appl. Mater. Interfaces* 5 (2013) 3614-3624.
- [30] A. Saravanan *et al.*, Fast growth of ultrananocrystalline diamond films by bias-enhanced nucleation and growth process in CH₄/Ar plasma, *Appl. Phys. Lett.* 104 (2014) 181603-5.
- [31] C. S. Wang, H. C. Chen, H. F. Cheng, I –N. Lin, Origin of platelike granular structure for the ultrananocrystalline diamond films synthesized in H₂ - containing Ar / CH₄ plasma, *J. Appl. Phys.* 107 (2014) 034304-7.
- [32] H. Zeng *et al.*, Boron-doped ultrananocrystalline diamond synthesized with an H-rich/Ar-lean gas system, *Carbon* 84 (2015) 103-117.
- [33] K. J. Sankaran, K. Panda, B. Sundaravel, H. –C. Chen, I –N. Lin, C. –Y. Lee, N. –H. Tai, Engineering the Interface Characteristics of Ultrananocrystalline Diamond Films Grown on Au-Coated Si Substrates, *ACS Appl. Mater. Interfaces* 4 (2012) 4169-4176.
- [34] J. P. Thomas *et al.*, Preferentially Grown Ultrananocrystalline Diamond and n-Diamond Grains on Silicon Nanoneedles from Energetic Species with Enhanced Field-Emission Properties, *ACS Appl. Mater. Interfaces* 4 (2012) 5103-5108.
- [35] K. J. Sankaran, H. –C. Chen, K. Panda, B. Sundaravel, C. –Young Lee, N. –H. Tai, I –N. Lin, Enhanced Electron Field Emission Properties of Conducting Ultrananocrystalline Diamond Films after Cu and Au Ion Implantation, *ACS Appl. Mater. Interfaces* 6 (2014) 4911-4919.
- [36] K. J. Sankaran, K. Panda, B. Sundaravel, N. H. Tai, I –N. Lin, Enhancing electrical conductivity and electron field emission properties of ultrananocrystalline diamond films by copper ion implantation and annealing, *J. Appl. Phys.* 115 (2014) 063701-7.

- [37] K. J. Sankaran *et al.*, Electron Field Emission Enhancement of Vertically Aligned Ultrananocrystalline Diamond-Coated ZnO Core–Shell Heterostructured Nanorods, *Small* 10 (2014) 179-185.
- [38] Y. Tzeng, S. Yeh, W. C. Fang, Y. Chu, Nitrogen-incorporated ultrananocrystalline diamond and multi-layer-graphene-like hybrid carbon films, *Sci. Rep.* 4 (2014) 4531.
- [39] S. C. Lin *et al.*, The microstructural evolution of ultrananocrystalline diamond films due to P ion implantation and annealing process-dosage effect, *Diam. Relat. Mater.* 54 (2015) 47-54.
- [40] K. Panda, E. Inami, Y. Sugimoto, K. J. Sankaran, I –Nan Lin. Straight imaging and mechanism behind grain boundary electron emission in Pt-doped ultrananocrystalline diamond films. *Carbon* 111 (2017) 8-17.
- [41] A. Saravanan, B. R. Huang, K. J. Sankaran, G. Keiser, J. Kurian, N. H. Tai, I. N. Lin, Structural modification of nanocrystalline diamond films via positive/negative bias enhanced nucleation and growth processes for improving their electron field emission properties, *J. Appl. Phys.* 117 (2015) 215307-11.
- [42] D. M. Gruen, S. Liu, A. R. Krauss, X. Pan, Buckyball microwave plasmas: Fragmentation and diamond-film growth, *J. Appl. Phys.* 75 (1994) 1758-1763.
- [43] P. Kovarik, E. B. D. Bourdon, R. H. Prince, Electron-energy-loss characterization of laser-deposited *a*-C, *a*-C:H, and diamond films, *Phys. Rev. B* 48 (1993) 12123-12129.
- [44] W. A. Yarbrough, R. Messier, Current issues and problems in the chemical vapor deposition of diamond, *Science* 247 (1990) 688-696.
- [45] R. J. Nemanich, J. T. Glass, G. Lucovsky, R. E. Shroder, Raman scattering characterization of carbon bonding in diamond and diamondlike thin films, *J. Vac. Sci. Technol. A* 6 (1988) 1783-1787.
- [46] R. E. Shroder, R. J. Nemanich, J. T. Glass, Analysis of the composite structures in diamond thin films by Raman spectroscopy, *Phys. Rev. B* 41 (1990) 3738-3745.
- [47] A. C. Ferrari, J. Robertson, Origin of the 1150cm^{-1} Raman mode in nanocrystalline diamond, *Phys. Rev. B* 63 (2001) 121405-5.
- [48] I. Jiménez, M. M. García, J. M. Albella, L. J. Terminello, Orientation of graphitic planes during the bias-enhanced nucleation of diamond on silicon: An x-ray absorption near-edge study, *Appl. Phys. Lett.* 73 (1998) 2911-2913.

- [49] J. Birrell, J. E. Gerbi, O. Auciello, J. M. Gibson, J. Johnson, J. A. Carlisle, Interpretation of the Raman spectra of ultrananocrystalline diamond, *Diam. Relat. Mater.* 14 (2005) 86-92.
- [50] R. Haubner, M. Rudigier, Raman characterisation of diamond coatings using different laser wavelengths, *Physics Procedia* 46 (2013) 71-78.
- [51] S. C. Ray, I –N. Lin, Ferroelectric behaviours of ultra-nano-crystalline diamond thin films, *Surf. Coat. Technol.* 271 (2015) 247-250.
- [52] Q. Huang *et al.*, Nanotwinned diamond with unprecedented hardness and stability, *Nature* 510 (2014) 250-253.
- [53] R. Y. Yakovlev *et al.*, Determination of impurities in detonation nanodiamonds by gamma activation analysis method, *Diam. Relat. Mater.* 55 (2015) 77-86.

Authors' biography:

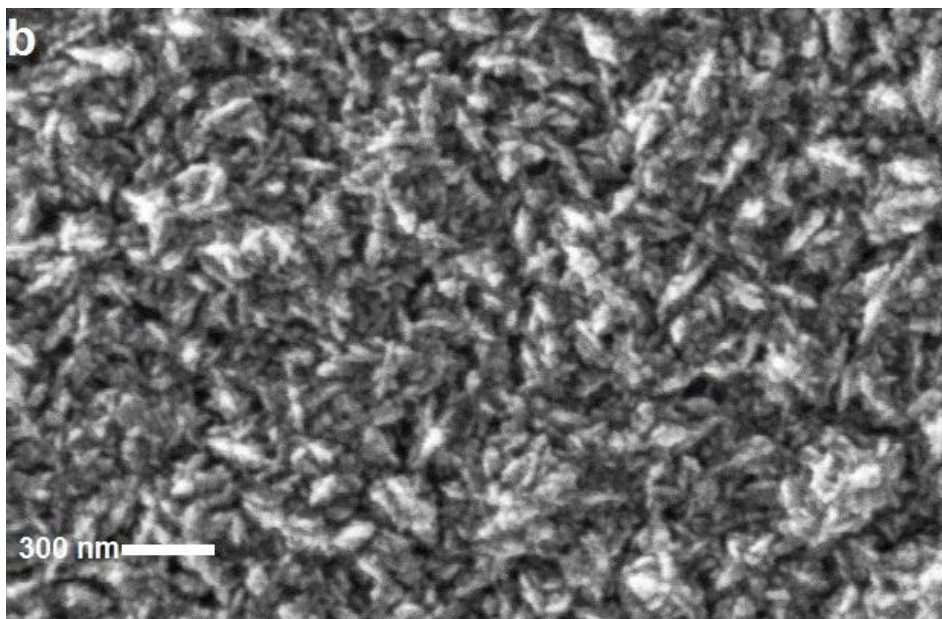
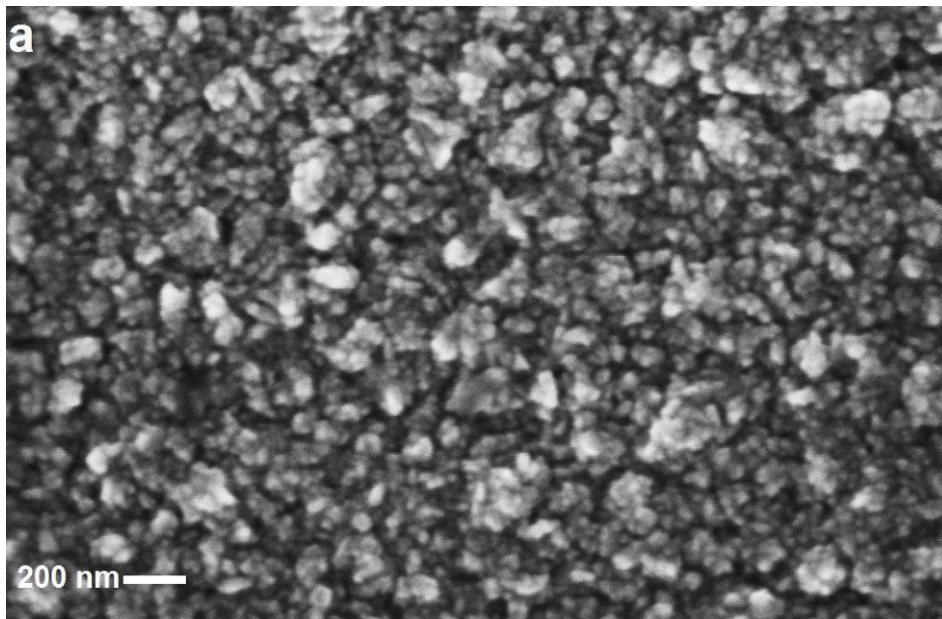


Mubarak Ali graduated from University of the Punjab with B.Sc. (Phys& Maths) in 1996 and M.Sc. Materials Science with distinction at Bahauddin Zakariya University, Multan, Pakistan (1998); thesis work completed at Quaid-i-Azam University Islamabad. He gained Ph.D. in Mechanical Engineering from Universiti Teknologi Malaysia under the award of Malaysian Technical Cooperation Programme (MTCP;2004-07) and postdoc in advanced surface technologies at Istanbul Technical University under the foreign fellowship of The Scientific and Technological Research Council of Turkey (TÜBİTAK; 2010). He completed another postdoc in the field of nanotechnology at Tamkang University Taipei (2013-2014) sponsored by National Science Council now M/o Science and Technology, Taiwan (R.O.C.). Presently, he is working as Assistant Professor on tenure track at COMSATS Institute of Information Technology, Islamabad campus, Pakistan (since May 2008) and prior to that worked as assistant director/deputy director at M/o Science & Technology (Pakistan Council of Renewable Energy Technologies, Islamabad; 2000-2008). He was invited by Institute for Materials Research (IMR), Tohoku University, Japan to deliver scientific talk on growth of synthetic diamond without seeding treatment and synthesis of tantalum carbide. He gave several scientific talks in various countries. His core area of research includes materials science, physics & nanotechnology. He was also offered the merit scholarship (for PhD study) by the Government of Pakistan but he couldn't avail. He is author of several articles published in various periodicals (<https://scholar.google.com.pk/citations?hl=en&user=UYjvhDwAAAAJ>).



I-Nan Lin is a senior professor at Tamkang University, Taiwan. He received the Bachelor degree in physics from National Taiwan Normal University, Taiwan, M.S. from National Tsing-Hua University, Taiwan, and the Ph.D. degree in Materials Science from U. C. Berkeley in 1979, U.S.A. He worked as senior researcher in Materials Science Centre in Tsing-Hua University for several years and now is faculty in Department of Physics, Tamkang University. Professor Lin has more than 200 referred journal publications and holds top position in his university in terms of research productivity. Professor I-Nan Lin supervised several PhD and Postdoc candidates around the world. He is involved in research on the development of high conductivity diamond films and also on the transmission microscopy of materials.

Supplementary Materials:



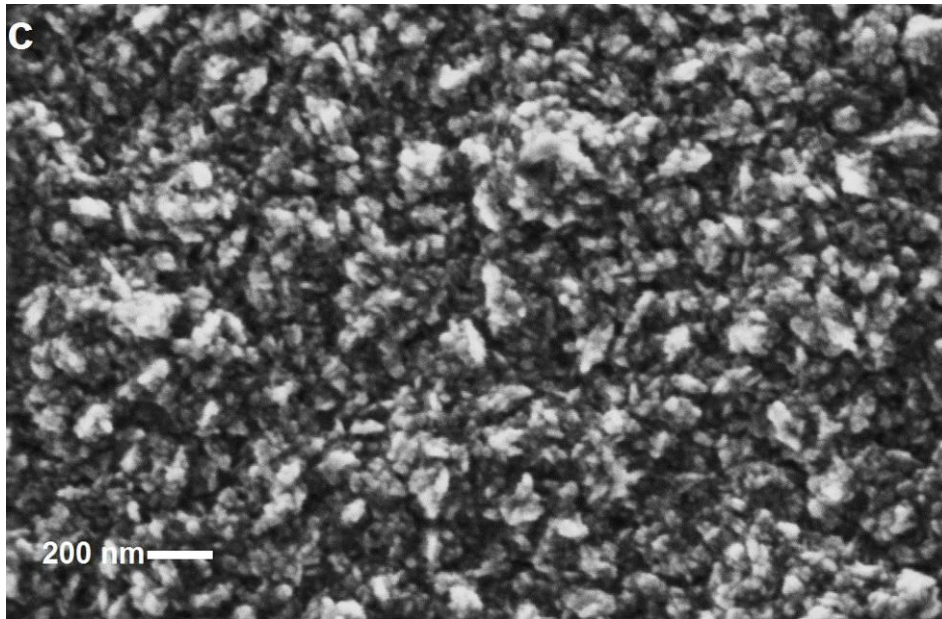


Figure S1: Surface morphology of 'tiny grains carbon films' synthesized at chamber pressure (a) 100 torr, (b) 150 torr, and (c) 200 torr; total mass flow rate: 200 sccm (6% H₂, 1 % CH₄ and 93 % argon, Ar: CH₄: H₂ = 186:2:12), microwave power: 1400 (in watts) and deposition time: 60 minutes.

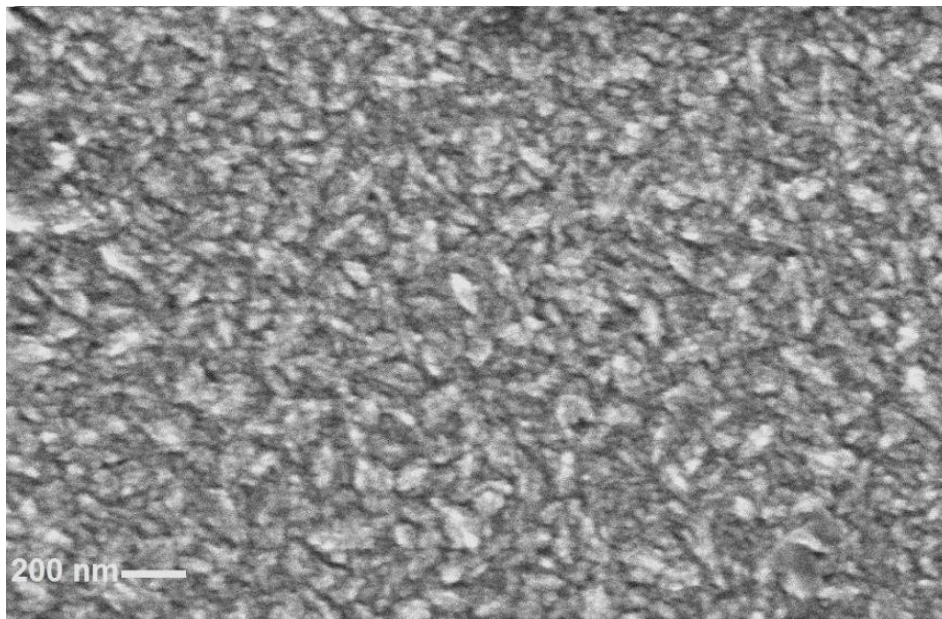


Figure S2: Surface morphology of 'tiny grains carbon film' synthesized at chamber pressure 150 torr; total mass flow rate: 200 sccm (0% H₂, 2 % CH₄ and 98 % argon, Ar: CH₄: H₂ = 196:4:0), microwave power: 1100 (in watts) and deposition time: 60 minutes.

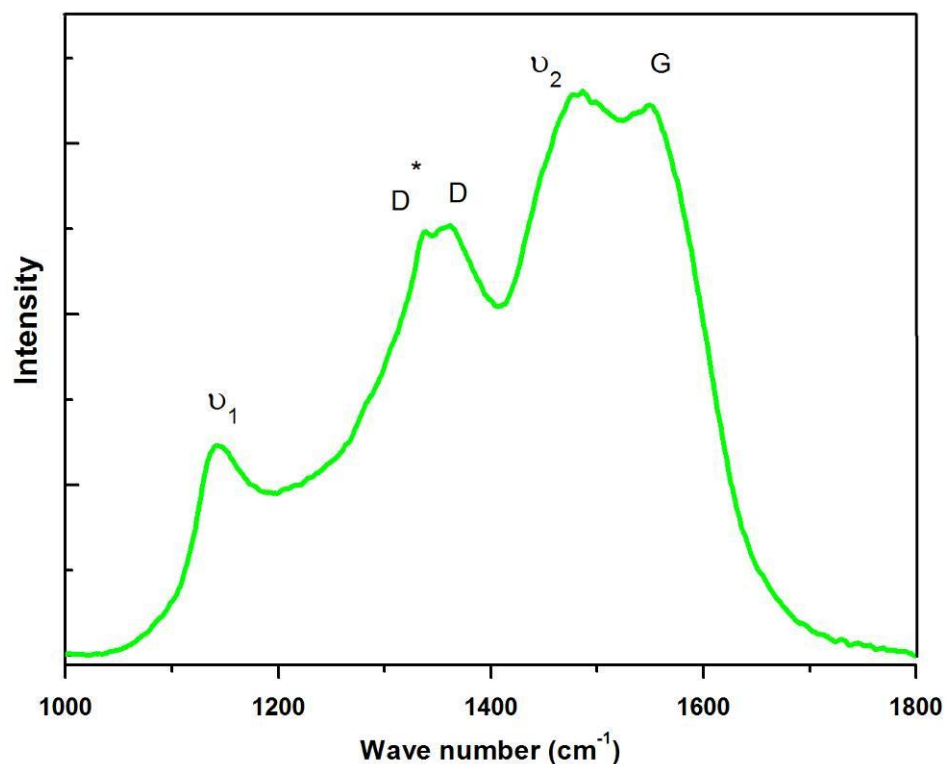
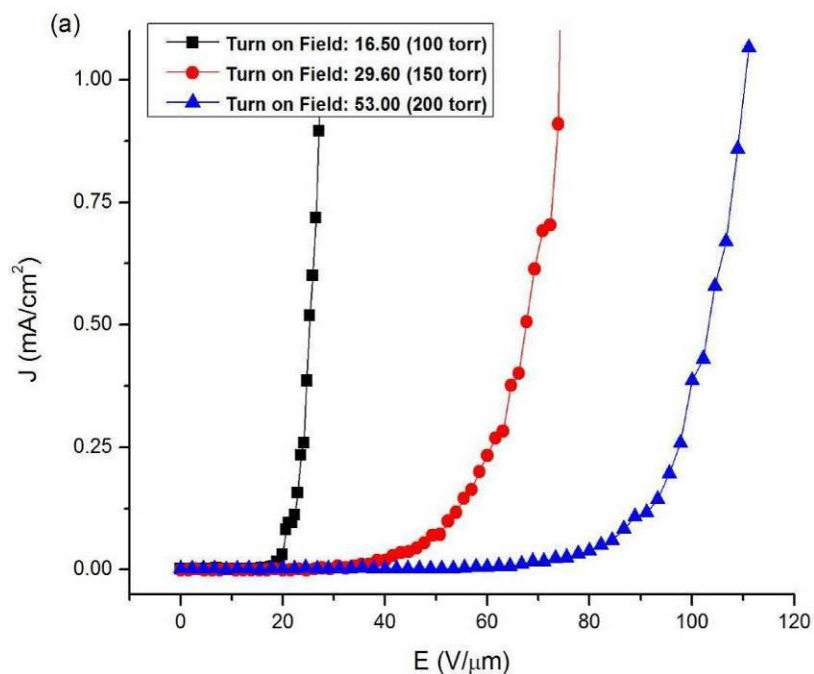


Figure S3: Raman spectrum of ‘tiny grains carbon film’ synthesized at chamber pressure 150 torr; total mass flow rate: 200 sccm (0% H₂, 2 % CH₄ and 98 % argon, Ar: CH₄: H₂ = 196:4:0), microwave power: 1100 (in watts) and deposition time: 60 minutes (ν_1 : ~ 1145 cm⁻¹, D*: ~ 1310 cm⁻¹, D: 1332 cm⁻¹, ν_2 : ~ 1480 cm⁻¹, G: ~ 1580 cm⁻¹).



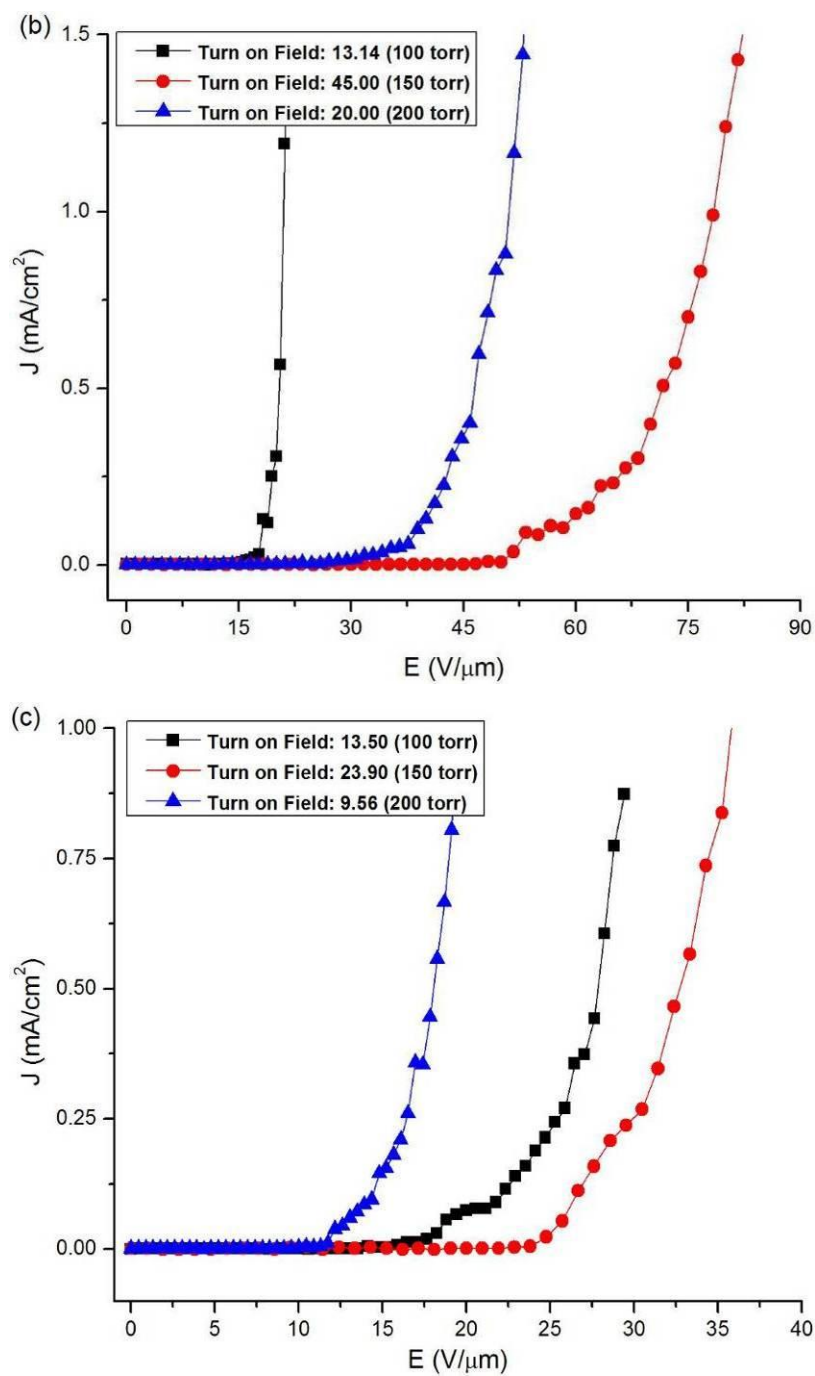


Figure S4: Field emission current density as a function of applied field of 'tiny grains carbon films' synthesized (a) without H₂, (b) with 3 % H₂ and (c) with 6 % H₂; 1 % CH₄, total mass flow rate: 200 sccm, microwave power: 1200 (in watts) and deposition time: 60 minutes.

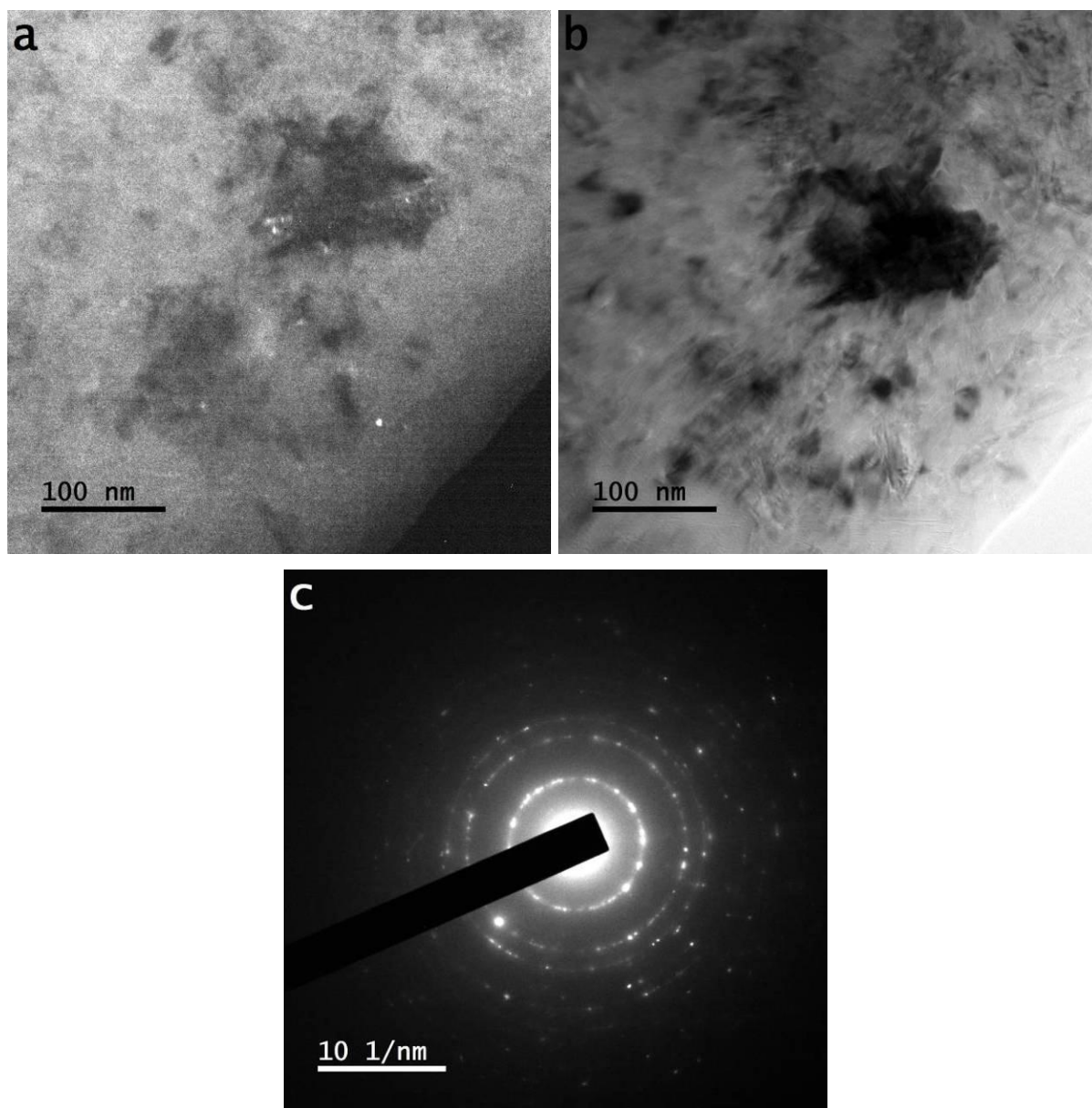


Figure S5: (a) Dark field transmission microscope image (b) bright field transmission microscope image and (c) SAPR pattern of 'tiny grains carbon film' synthesized at chamber pressure: 100 torr, total mass flow rate: 200 sccm (6% H₂, 1 % CH₄ and 93 % argon), microwave power: 1400 watts (in watts) and deposition time: 60 minutes.

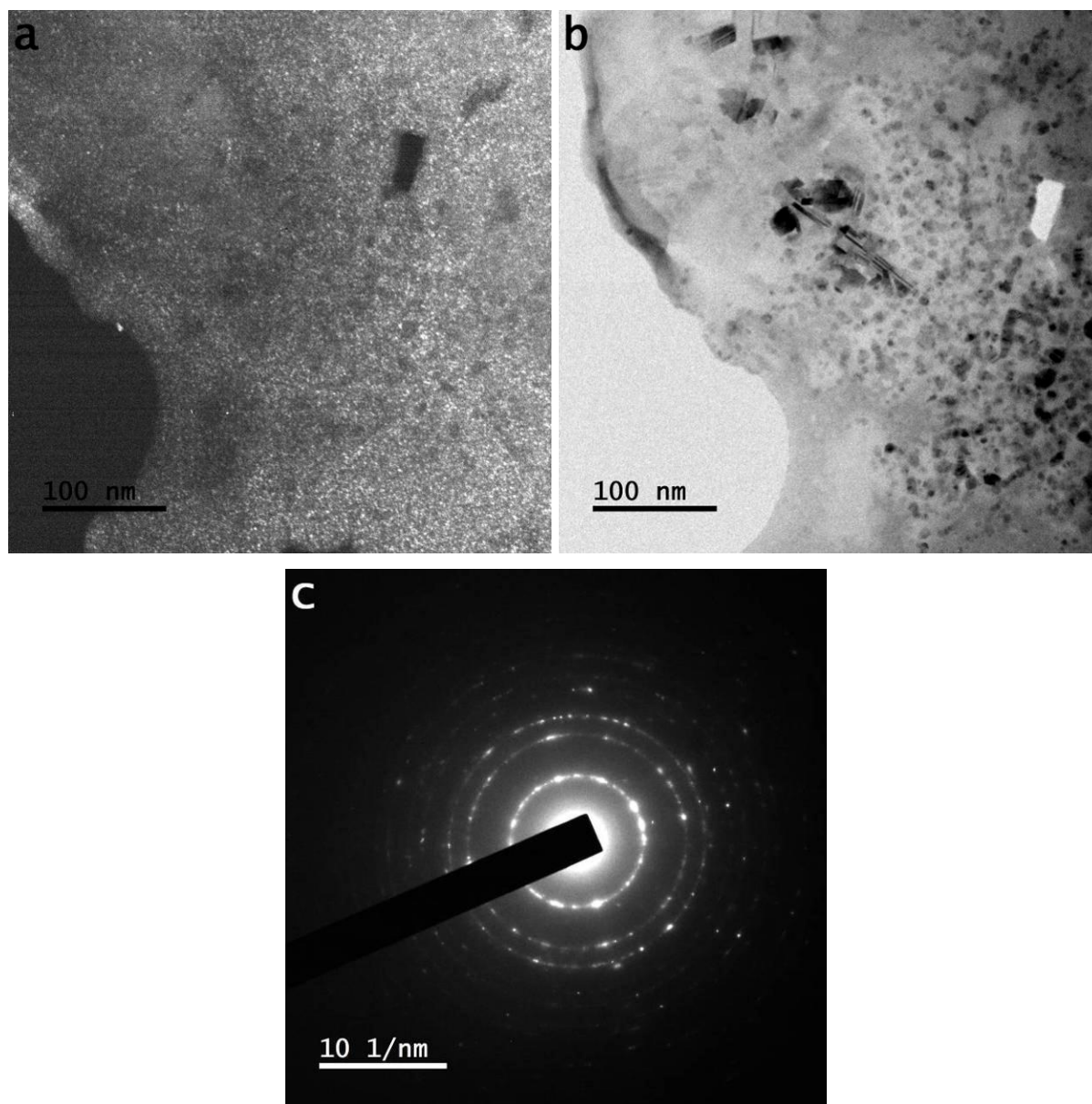


Figure S6: (a) Dark field transmission microscope image (b) bright field transmission microscope image and (c) SAPR pattern of 'tiny grains carbon film' synthesized at chamber pressure: 200 torr, total mass flow rate: 200 sccm (6% H₂, 1 % CH₄ and 93 % argon), microwave power: 1400 (in watts) and deposition time: 60 minutes.

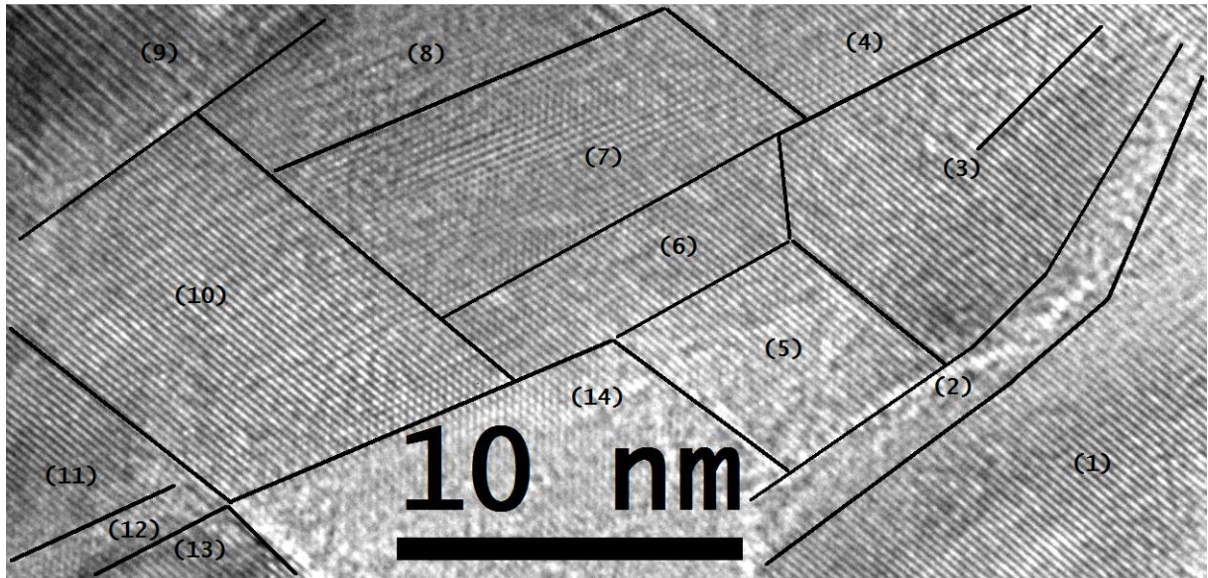


Figure S7: High resolution transmission microscope image of 'tiny grains carbon film' synthesized at chamber pressure 100 torr shows different modified phases of tiny grains; total mass flow rate: 200 sccm (6% H₂, 1 % CH₄ and 93 % argon), microwave power: 1400 (in watts) and deposition time: 60 minutes.